

# Interface Structure and Corrosion Resistance of Ti/Cr Nanomultilayer Film Prepared by Magnetron Sputtering on Depleted Uranium

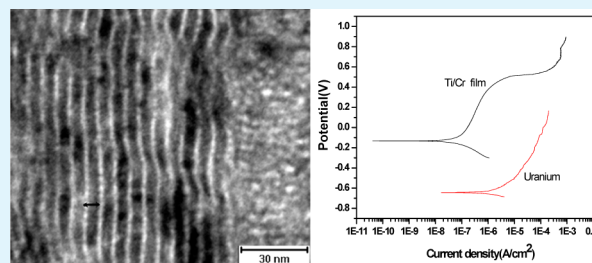
Shengfa Zhu,<sup>†,\*</sup> Yanping Wu,<sup>†</sup> Tianwei Liu,<sup>‡</sup> Kai Tang,<sup>†</sup> and Qiang Wei<sup>†</sup>

<sup>†</sup>China Academy of Engineering and Physics, Mianyang, P.R. China

<sup>‡</sup>Science and Technology on Surface Physics and Chemistry Laboratory, Mianyang, P.R. China

**ABSTRACT:** Uranium has broadened utility in military and civilization; however, it is extremely apt to oxidation corrosion. Ti/Cr nanomultilayer film was prepared by unbalanced magnetron sputtering on the surface of depleted uranium (DU) to improve its corrosion resistance. The SEM morphologies show that Ti/Cr multilayer film has fine grain and high density. The Auger electron spectroscopy is used to investigate the depth profiles of Ti, U, and O elements of interface between DU substrate and the Ti interlayer, and indicates that the mutual diffusion area of U and Ti is formed at the interface. The TEM cross-section microstructure shows that the multilayer film has alternative Ti and Cr layers and form a perfect modulation structure. The modulation period is measured to be 4.8 nm in TEM morphology, the thickness ratio of Ti to Cr could be estimated to be about 1:2. Potentiodynamic polarization curves show that, after depositing Ti/Cr nanomultilayer film, the corrosion potential increases while the corrosion current density decreases obviously. The surface of Ti/Cr nanomultilayer film exhibits a pseudo passivation behavior when the polarization potential increased from  $-50$  to  $400$  mV. It was indicated that, after depositing Ti/Cr nanomultilayer film by unbalanced magnetron sputtering, the corrosion resistance of DU was effectively improved.

**KEYWORDS:** depleted uranium, unbalanced magnetron sputtering, nanomultilayer film, corrosion resistance



## 1. INTRODUCTION

Depleted uranium (DU) has both military and civilian applications. Because of its high density, DU is mainly used in high density penetrators, inertial guidance systems, gyroscopic compasses,<sup>1</sup> nuclear fuel, and so on. However, uranium is extremely apt to oxidation corrosion because of its high chemical activity, especially in salty, humid, and high-temperature environments.<sup>2,3</sup> The corrosion of uranium can shorten the lifetime of components, whereas the corrosion products can release airborne particles that present environmental and health hazards. To reduce the corrosion, we have used surface modifications and various coating methods to produce environmentally friendly corrosion resistant coatings on the uranium. Sacrificial zinc coatings, arc plasma and vapor deposited Al-based coatings,<sup>4,5</sup> Ti-based coatings,<sup>6,7</sup> and  $N^+$  and  $C^+$  ion implantation<sup>8,9</sup> have been investigated. In the present investigation, nanomultilayer coatings have been widely studied because of their promising properties. These coatings possess an unusual combination of mechanical and chemical properties, such as high fracture toughness, high cracking resistance, good corrosion resistance, and high thermal and chemical stability.<sup>10–12</sup> The single layer, such as Ti or TiN, is columnar structure, and easily form pore and crack, which could decrease the corrosion resistance of substrate. The multilayer coatings have the different alternative structure, and produced a lot of microinterface, which could restrain the growth of columnar crystal, decrease the opportunity of pore formation, and increase the density of coatings. Thus, we decide to prepare

to multilayer coatings and study their microstructure and properties. Superhard coatings, such as TiN CrN, are widely used in the tool and mold fields. Although these hard-wearing coatings have many advantages, they still have much higher residual stress, which could deduce to the pilling off of coatings. The metal coatings (Ti or Cr) have much low hardness, and the stress of Ti/Cr multilayer is lower than those of nitride coatings. So the Ti/Cr multilayer was chosen to on the surface of uranium.

Unbalanced magnetron sputtering is one of the PVD coating techniques and is widely used in the production of superhard coatings, corrosion resistance coatings, and other functional coatings. An unbalanced magnetron possesses stronger magnets on the outside resulting in the expansion of the plasma away from the surface of the target toward the substrate. The magnets form an electron trap to increase the level of ionization. When a negative bias is applied to the substrate, ions are accelerated and bombard the substrate, and effectively improve the properties of the coatings. So in this study, the unbalanced magnetron sputtering techniques was used to synthesize nanoscale Ti/Cr multilayer film on the surface of DU. The structure and corrosion resistance of the Ti/Cr film on uranium were investigated. The surface morphology and the depth profiles of elements were analyzed by SEM and Auger

Received: April 8, 2013

Accepted: June 19, 2013

Published: June 19, 2013

energy spectroscopy (AES), respectively. The interface microstructure of Ti/Cr multilayer film was examined by cross-sectional TEM. The corrosion behavior of the samples was evaluated using potentiodynamic polarization curves.

## 2. EXPERIMENTAL DETAILS

**2.1. Sample Preparation.** The Ti/Cr nanomultilayer film was deposited in medium frequency unbalanced magnetron sputter (MFUMS) chamber. The schematic of our system is shown in Figure 1. The pure Ti (99.95%) and Cr (99.95%) targets were positioned

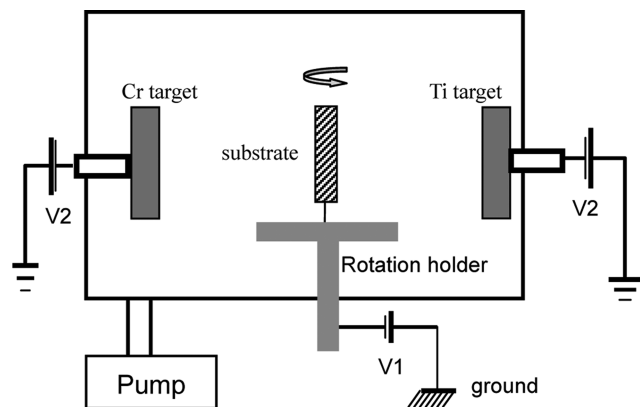


Figure 1. Schematic diagram of the deposition system.

symmetrically around the samples at distance of 150 mm. Substrate are Si (100) wafer and depleted uranium (DU) disk with the diameter of 15 mm and the thickness of 3 mm. The Si (100) wafer substrates were used to analyze cross-sectional morphologies. The DU samples were abraded with up to 1000-grit SiC water paper and mechanically polished with 0.5  $\mu\text{m}$  diamond paste, then ultrasonically cleaned progressively in acetone and ethanol for 5 min, respectively. To reduce contaminations, the samples were immediately put into vacuum chamber and started pumping. The base pressure was lower than  $5 \times 10^{-4}$  Pa.

Prior to coating deposition, the substrates were cleaned by  $\text{Ar}^+$  glow discharge plasma at a bias of  $-800$  V for 10 min to remove the native oxide scale. After presputtering, about 100 nm thickness Ti buffer layer was first deposited on substrates to enhance coatings adhesion. During deposition, high purity Argon was introduced and controlled using mass flow controllers. The Ar gas flow was kept at 100 sccm. The work pressure was  $4 \times 10^{-1}$  Pa. The pulse bias voltage of  $-1000$  V, with frequency of 40 kHz and duty cycle of 15%, was applied to the substrate. During Ti/Cr coating depositing, alternative Ti and Cr layers were obtained by adjusting the time exposing the substrates to the Ti and Cr targets. A pulse voltage of  $-300$  V, superimposed on DC of  $-50$  V, was applied to the substrate. At the same time, the target current of Ti and Cr was hold at 3 A. Stueber<sup>13</sup> and Sun<sup>14</sup> reported that when the modulation periods were in the range of 2–10 nm, nanomultilayer film showed superlattice effect and had good corrosion resistance. So Ti/Cr multilayer film with modulation period of 8 nm was designed. According to the test, the growth rates of Ti and Cr film were 0.16 and 0.34 nm/s, respectively. In this experiment, the sample holder was rotated at a speed of 2 rpm. That is, each of the Ti and Cr layers was deposited in about 15 s, and 50 min after deposition, the number of layers in multilayer was about 100 cycles. Synthesis parameters of Ti/Cr coatings by MFUMS were listed in Table 1.

**2.2. Surface Characterizations.** The microstructure of Ti/Cr multilayer film was observed using scanning electron microscopy operated at 15 kV. Film thickness was measured by examining SEM cross-sectional images.

AES depth profiles were used to analyze the distribution of U, Ti, O, C elements in the interface between uranium substrate and Ti interlayer. AES instrument model is PHI650 SAM, that excitation

Table 1. Experimental Parameters of Ti/Cr Coating Preparation

deposition parameters	conditions
base pressure	$5.0 \times 10^{-4}$ Pa
$\text{Ar}^+$ presputter cleaning	$-800$ V $\times$ 60%, 10 min
Ti target current	3 A
Cr target current	3 A
Ar flux	100 sccm
Ti interlayer	$-1000$ V $\times$ 15%, 10 min
Ti/Cr deposition bias	$-300$ V $\times$ 15%+DC 50 V
work pressure	$4 \times 10^{-1}$ Pa
deposition time	50 min
sample rotated speed	2 rpm
temperature of substrate	$200 \pm 5$ $^{\circ}\text{C}$

energy is 3 keV, electron beam current is 100 nA, energy of  $\text{Ar}^+$  is 4 keV, sputtering area is 1  $\text{mm}^2$ .

The cross-sectional structure and morphology of the Ti/Cr multilayer was performed with transmission electron microscopy (TEM) on F20 operating at 200 kV. The TEM specimens were prepared by cutting the films together with substrates in cross-section and were mechanically polished to be less than 100  $\mu\text{m}$ , then milled from both sides by ions to be the thickness for TEM observation.

**2.3. Electrochemical Corrosion Test.** The corrosion behavior of Ti/Cr multilayer film was investigated on EG&G M273 electrochemical workstation. The potentiodynamic polarization curves (E/I) were measured in a three-electrode cell with a Luggin capillary; a platinum slice as counter electrode, and a saturated calomel electrode (SCE) was chosen as reference electrode. The experiments were performed in a 0.05 wt %  $\text{Cl}^-$  corrosion solution. The effective area of the samples was about 1  $\text{cm}^2$ . Before testing, the samples were dipped in the solution for about 60 min until the open circuit potential became stable with a fluctuation of  $\pm 5$  mV. Then the polarization curves (E/I) were obtained by scanning from the potential of  $-700$  mV to 1000 mV with respect to the SCE with a scan rate of 2 mV/s.

## 3. RESULTS AND DISCUSSION

The surface and cross-sectional morphologies of nanoscale Ti/Cr multilayered coatings prepared by unbalanced magnetron sputtering at bias voltage of  $-300$  V was showed in Figure 2.

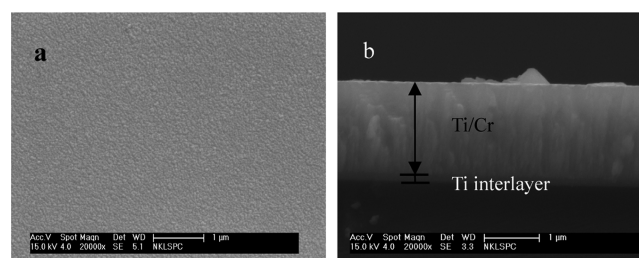
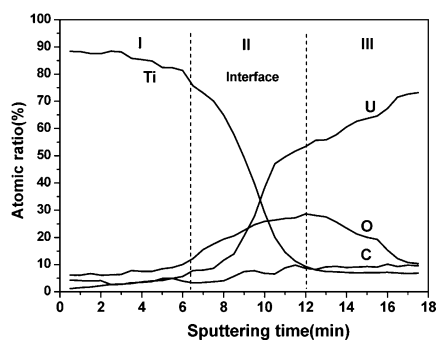


Figure 2. (a) Surface and (b) cross-section morphologies of Ti/Cr nanomultilayer coating.

Figure 2a showed the surface morphology with FE SEM. The microstructure of Ti/Cr surface was densely packed, no voids and microparticles. To improve the adhesion between coatings and substrate, a layer of Ti interlayer was prepared at a higher pulse bias voltage of  $-1000$  V before depositing Ti/Cr multilayer film. From Figure 2b, it is found that the coatings were composed of two parts, one was Ti interlayer, and the other was Ti/Cr multilayer coatings. The Ti interlayer was very compact and there were no micro cracks and visible voids. The thickness of Ti interlayer was approximately 100 nm. Because the unbalanced magnetic field could trap fast moving secondary

electrons, it could increase the opportunity of electrons collision with neutral gas atoms away from the target surface, which could produce a great number of metal ions. When a negative bias was applied to the substrate, positive metal ions from the plasma were accelerated to the substrate and bombard it; these ions bombardment could make the physically adsorbed atoms with lower adhesion sputtered and the particles with higher adhesion rammed down further. The higher the bias voltage, the stronger the ion bombardment. The bias voltage of  $-1000$  V could effectively improve the adhesion between substrate and coatings. A typical SEM cross-sectional morphology of a Ti/Cr multilayered coating prepared at bias voltage of  $-300$  V was illustrated in Figure 2b. It can be seen that the Ti/Cr coating restrained the growth of columnar grains; its microstructure was uniform and compact. Because the modulation period was very small, the interface of Ti layer and Cr layer did not distinguish with SEM even if the magnification was up to 20 thousand times.

A typical Auger profile of Ti film on uranium substrate was shown in Figure 3 reporting the elemental distribution of Ti, U,



**Figure 3.** Depth profiles of elements near interface between Ti interlayer and uranium substrate.

O, and C as a function of  $\text{Ar}^+$  sputtering time. Three zones can be identified: In zone I, the sample is cleaned from surface contamination (adsorbed species like C, O), a steady state is reached after a certain sputtering time. In zone II the interface between the Ti film and uranium substrate is reached, characterized by the decrease of the titanium and increase of the oxygen and uranium signal. The original formation of the oxygen at the interface was possibly derived from the surface oxidation corrosion of uranium. Because the chemical nature of depleted uranium is very active and apt to oxidation corrosion

in natural environment. Therefore, a layer of uranium oxides was formed on the surface of uranium before depositing Ti interlayer. As a result, there was a higher atomic ratio of oxygen element in zone II. Zone III represents the substrate. Because of an interaction of the sputtering ions with the surface atoms are not only removed from the surface but also knocked into the sample. This leads to atomic mixing and broadening of the surface oxide layer. Thus, in zone III, the content of oxygen element was still higher, but rapidly decreased with the prolongable sputtering time. The presence of oxygen element in zone II and zone III might reduce the adhesion between Ti/Cr nanomultilayer and uranium substrate and decrease the depleted uranium corrosion protection performance.

The AES differential spectrum of uranium is different with its oxides. Idriss<sup>15</sup> characterized the  $\text{UO}_2$  (111) single crystal with AES and found that the peak energy of  $\text{UOPV}$ ,  $\text{UO}_5\text{VV}$ , and  $\text{UO}_4\text{VV}$  of  $\text{UO}_2$  was 73, 84, and 94 eV, respectively. Jiang<sup>16</sup> et al. prepared the uranium thin films at  $1 \times 10^{-6}$  Pa and found that the Auger peak energy of  $\text{UOPV}$ ,  $\text{UO}_5\text{VV}$ , and  $\text{UO}_4\text{VV}$  of uranium was 74.8, 90, and 98 eV using AES in situ characterization, which showed that the peak energy of metal uranium was higher than that of uranium oxides. Figure 4 showed the higher-resolution AES spectra of uranium and titanium elements at different depth in Ti/U interface. From Figure 4a, it was found that the peak of  $\text{UOPV}$  started to appear when  $\text{Ar}^+$  sputtered 5 min, the peak energy of  $\text{UOPV}$  was 74.5 eV. With the increased of  $\text{Ar}^+$  sputtering time, the characteristic peak of  $\text{UO}_5\text{VV}$  and  $\text{UO}_4\text{VV}$  gradually appeared and their corresponding peak energy were 84.5 eV and 95.5 eV respectively. These results were similar to the reports of Idriss. When  $\text{Ar}^+$  sputtering time was between 5 min to 14 min, the uranium characteristic peak of 90.5 eV coexists with the peak of 84.5 eV and 95.5 eV, which showed that a part of uranium existed in oxidation state and another part of uranium existed in metal state. After  $\text{Ar}^+$  sputtering 16 min, the Auger peak of uranium oxidation state at 84.5 eV and 95.5 eV disappeared, at the same time, the peak at 98.5 eV appeared. This indicated the chemical state of uranium transform from oxidation state into metal state. Figure 4b showed the Auger spectra of titanium as the  $\text{Ar}^+$  sputtering time. The characteristic peak of Ti at 418 eV did not disappear until  $\text{Ar}^+$  sputtering 14 min. From Figure 4, the elements of Ti and U coexisted when  $\text{Ar}^+$  sputtering time was between 5 to 14 min, that is to say, a mutual diffusion area of uranium and titanium was formed at the interface of Ti/U.

Figure 5 showed the cross-section TEM morphology of the Ti/Cr nanomultilayer. It can be seen that the multilayer had a

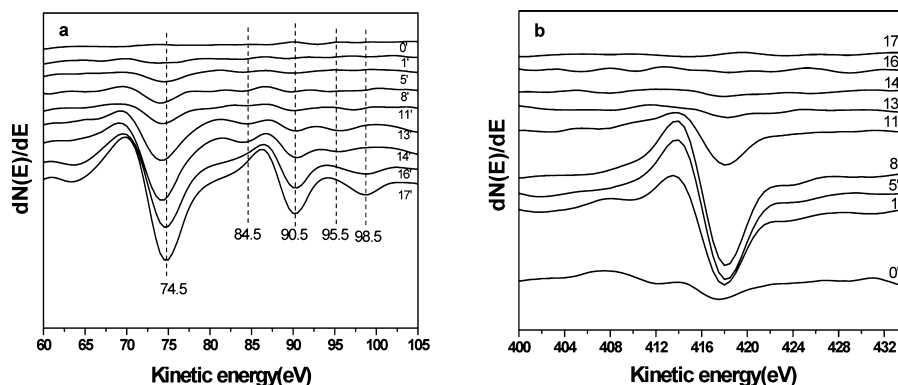


**Figure 4.** Differential spectra of (a) U and (b) Ti at different depth in Ti/U interface.

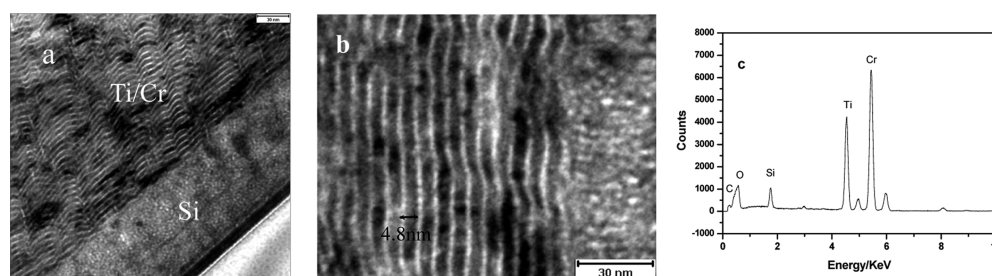


**Figure 5.** Cross-section TEM micrograph of (a, b) Ti/Cr nanomultilayer film and (c) EDS pattern.

perfect modulation structure with bilayers. Energy-dispersive spectroscopy (EDS) examination showed that the multilayer film was mainly composed of Ti and Cr elements, only existed a small number of C and O elements, as shown in Figure 5c. The intensity of Cr was much higher than Ti element, and the relative intensity ratio of Cr to Ti was about 1.7 to 1. The carbon and oxygen elements on the surface of the samples probably came from the process of rinsing with acetone and ethanol and from the contaminants in air. TEM examination revealed that the multilayer had alternative Ti and Cr layers in a different thickness; the Ti layers had a thickness much smaller than Cr layers in the multilayer film. The modulation period, that is the thickness of single layer of Ti and Cr films, was measured to be about 4.8 nm in the cross-section TEM of the multilayer. The ratio in thickness could be estimated to be about 2:1 for Cr layer to Ti layer. This result was similar to the EDS relative intensity ratio of Cr to Ti.

Figure 6 showed the potentiodynamic polarization curves of the nanoscale Ti/Cr multilayered film and untreated DU.

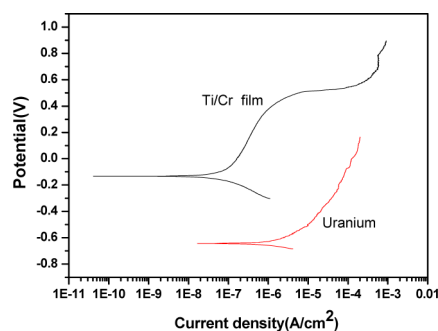


**Figure 6.** Polarization curves of Ti/Cr multilayer and as-deposited DU.

Before the test, the samples were immersed in the 0.05 wt %  $\text{Cl}^-$  corrosion solution for 60 min. As can be seen in the figure, the corrosion potential of untreated DU was about  $-641$  mV vs SCE determined by extrapolation of Tafel region. After a layer of Ti/Cr nanomultilayer film was deposited, the corrosion potential increased about 500 mV, whereas the corrosion current density decreased at least 2 orders of magnitude. The lower the corrosion current density in the polarization area, the better the corrosion resistance. At free-corrosion potential nearby, the polarization current of the multilayer film rapidly increased with the increasing polarization potential. This showed the electrode reaction process was controlled by active polarization of electron transformation. When the polarization potential increased from  $-50$  to 400 mV, the slope of the anode polarization increased and the rate of the increase in the polarization current decreased, which indicated that the

resistance of electrode reaction process increased and electron transfer could be restrained. These results were similar to the studies of Liu,<sup>7</sup> where Ti/TiN multilayer protective coatings were prepared on uranium and its corrosion potential increased by 580 mV. The surface of Ti/Cr nanomultilayer film exhibited a pseudo passivation behavior marked by a small increase in the current density at higher potentials. When the potential polarization increased to about 700 mV, secondary passivation phenomenon appeared. Ti/Cr multilayered film could distinctively improve the corrosion resistance of DU, the reason might be that: (i) Alternating interlayers of different compositions could redirect the current flow between coating and substrate, and therefore increase the resistance of electron diffusion and migration between in metal conductor (Ti/Cr nanomultilayer film) and in ion conductor because of a large number of interfaces. (ii) Alternative deposition Ti and Cr elements produced a lot of microinterface, which could restrain the growth of columnar crystal, decrease the opportunity of pore formation and reduce the possibility of through-coating defects (e.g., micropores and microcracks). (iii) The crack starting from the coating surface might be split and deflect at the interface zone between the layers, which decreased the porosity and increased the density of coatings. Thus, the Ti/Cr film deposited on the surface of DU tended to be very protective and could effectively improve the surface corrosion resistance of DU.

#### 4. CONCLUSIONS

Ti/Cr nanoscale multilayer film was prepared on the surface of depleted uranium by unbalanced magnetron sputtering to improve its corrosion resistance. The multilayer film had alternative Ti and Cr layers in a different thickness, and had a perfect modulation structure with fine grain and high density. The modulation period was measured to be 4.8 nm and the ratio in thickness of Ti to Cr could be estimated to be about 1 to 2. AES results showed that Ti diffused into uranium substrate and formed a mutual diffusion group of U and Ti at the interface of Ti/U after depositing Ti interlayer. A large number of interfaces of Ti/Cr nanomultilayer film restrained the growth of columnar crystal, interrupted the penetrating defects of micro holes and micro cracks, decreased the porosity and increased the density of multilayer film. The surface of Ti/Cr nanomultilayer film exhibited a pseudo passivation behavior when the polarization potential increased from  $-50$  to 400 mV. It was showed that, after depositing Ti/Cr nanomultilayer film by unbalanced magnetron sputtering, the corrosion resistance of uranium was effectively improved. The influence of the presence of oxygen element in Ti interlayer on the adhesion between Ti/Cr nanomultilayer and uranium substrate need further investigate.

## AUTHOR INFORMATION

### Corresponding Author

\*E-mail: zhushf-306@163.com.

### Notes

The authors declare no competing financial interest.

## ACKNOWLEDGMENTS

This work was supported by China Academy of Engineering Physics Project of 2012B0302049.

## REFERENCES

- (1) Hammond, C. R. In *Handbook of Chemistry and Physics*, 81st ed.; Lide, D. R.; CRC Press: Boca Raton, FL, 2004; Vol. 4, pp 1–43.
- (2) Wilkinson, W. D.; *Uranium Metallurgy*; Interscience: Boston, 1962; pp 757–764
- (3) McGillivray, G. W.; Geeson, D. A.; Greenwood, R. C. *J. Nucl. Mater.* **1994**, *208*, 81–97.
- (4) Chang, F.; Levy, M.; Jackman, B.; Nowak, W. B. *Surf. Coat. Technol.* **1991**, *48*, 31–39.
- (5) Lv, X. C.; Wang, X. L.; Lang, D. M.; Dong, P. *Trans. Nonferrous Met. Soc. China* **2003**, *14*, 247–250.
- (6) Chang, F. C.; Levy, M.; Huie, R.; Kane, M.; Buckley, P.; Kattamis, T. Z.; Lakshminarayan, G. R. *Surf. Coat. Technol.* **1991**, *49*, 87–96.
- (7) Liu, T. W.; Dong, C.; Wu, S.; Tang, K.; Wang, J. Y.; Jia, J. P. *Surf. Coat. Technol.* **2007**, *201*, 6737–6741.
- (8) Arkush, R.; Mintz, M. H.; Kimmel, G.; Shamir, N. *J. Alloys Compd.* **2002**, *340*, 122–126.
- (9) Arkush, R.; Mintz, M. H.; Shamir, N. *J. Nucl. Mater.* **2000**, *281*, 182–190.
- (10) Chung, Y. W.; Sproul, W. D. *MRS Bull.* **2003**, *28*, 164–168.
- (11) Veprek, S.; Veprek-Heijman, M. G. J.; Karvankova, P.; Prochazka, J. *Thin Solid Films* **2005**, *476*, 1–29.
- (12) Bardi, U.; Chenakin, S. P.; Ghezzi, F.; Giolli, C.; Goruppa, A.; Lavacchi, A.; Miorin, E.; Pagura, C.; Tolstogousov, A. *Appl. Surf. Sci.* **2005**, *252*, 1339–1349.
- (13) Stueber, M.; Holleck, H.; Leiste, H.; Seemann, K.; Ulrich, S.; Ziebert, C. *J. Alloys Compd.* **2009**, *483*, 321–333.
- (14) Sun, P. L.; Hsu, C. H.; Liu, S. H.; Su, C. Y.; Lin, C. K. *Thin Solid Films* **2010**, *518*, 7519–7522.
- (15) Idriss, H. *Surf. Sci. Rep.* **2010**, *65*, 67–109.
- (16) Jiang, C. L.; Xian, X. B.; Xiao, H.; Lu, L.; Vac., J. *Sci. Technol. (China)* **2009**, *29*, 135–138.